Interference Modelling in a Multi-Cell LoRa System

Luca Beltramelli, Aamir Mahmood, Mikael Gidlund, Patrik Österberg and Ulf Jennehag
Mid Sweden University, Sundsvall SE-85170, Sweden
Email: {luca.beltramelli, aamir.mahmood, mikael.gidlund, patrik.osterberg, ulf.jennehag}@miun.se

***Abstract*—As the market for low-power wide-area network (LPWAN) technologies expands and the number of connected devices increases, it is becoming important to investigate the performance of LPWAN candidate technologies in dense deployment scenarios. In dense deployments, where the networks usually exhibit the traits of an interference-limited system, a detailed intra- and inter-cell interference analysis of LPWANs is required. In this paper, we model and analyze the performance of uplink communication of a LoRa link in a multi-cell LoRa system. To such end, we use mathematical tools from stochastic geometry and geometric probability to model the spatial distribution of LoRa devices. The model captures the effects of the density of LoRa cells and the allocation of quasi-orthogonal spreading factors (SF) on the success probability of the LoRa transmissions. To account for practical deployment of LoRa gateways, we model the spatial distribution of the gateways with a Poisson point process (PPP) and Matèrn hard-core point process (MHC). Using our analytical formulation, we find the uplink performance in terms of success probability and potential throughput for each of the available SF in LoRa's physical layer. Our results show that in dense multi-cell LoRa deployment with uplink traffic, the inter-cell interference noticeably degrades the system performance.**

I. Introduction

LoRa is a one of the rising stars of low-power wide-area network (LPWAN)-based IoT technologies [1]. LoRa is characterized by a long range, typically a few tens of kilometers, low data rates and low-energy consumption. Thanks to the large number of practical applications for LPWAN-IoT technologies in fields such as security, agriculture, smart metering and smart cities, LoRa is gaining popularity in industry and academia. Given the rapid growth of LoRa and that it operates in unlicensed bands, dense deployment scenarios will inevitably see the presence of neighboring LoRa cells.

LoRa technology consists of a proprietary physical (PHY) layer and a media access control (MAC) layer. To achieve long transmission distances with low transmit power, LoRa operates in the sub-1GHz band. At PHY, a proprietary modulation scheme by Semtech [2] based on chirp spread spectrum (CSS) is used. It supports six quasi-orthogonal spreading factors (SF) [2]. The MAC layer of LoRa is specified in the LoRaWAN, an open standard, developed and maintained by the LoRa Alliance [3]. LoRaWAN specifies two types of devices: LoRa gateway and LoRa end device (ED). The EDs are the sensors and actuators that needs to communicate with a LoRa server. A LoRa gateway is simply in charge of relaying the messages between the ED and the LoRa server. LoRa EDs, with a packet to transmit, randomly access the channel using a simple non-slotted ALOHA protocol.

Recently, many literature studies have analyzed and characterized the interference in a LoRa network [4]–[8]. A majority of the existing studies have only focused on modelling the interference in a single LoRa cell. In [5], a multi-cell LoRa network is analyzed using stochastic geometry where the authors assumed perfect orthogonality among the different spreading factors. However, the validity of such assumption was recently disproved in [7] where a simulation based study of a multi-cell LoRa network under quasi-orthogonal SFs was conducted. In their simulations, the authors considered 4 and 16 adjacent LoRa cells deployed in a regular grid. In general, developing a mathematical model of interference in cells deployed in a grid is complex, and leads to intractable formulation for which only approximation exists [9]. Moreover, grid-based models are inaccurate in realistic scenarios as they fail to account for a degree of randomness in the cells deployment.

To the best of the authors' knowledge, the prior work in the literature fails to analytically model the performance of a multi-cell network with the allocation of quasi-orthogonal SFs. In this paper, we address this gap by modelling the interference in a multi-cell LoRa system using the frameworks of stochastic geometry and geometric probability. Therein, to capture the randomness in the deployment of LoRa cells, we make use of stochastic geometry. The spatial distribution of the cells is modelled with two different point processes. In particular, a Poisson point process (PPP) is used for modelling the random and independent distribution of LoRa cells, whereas a Matèrn hard-core point process (MHC) is used to model a minimum distance between cells, typically found in cell planning. In accordance with the results presented in [7] and [8], in addition to modelling intra and inter-cell interference, our model incorporates the imperfect orthogonality between different SFs. The performance of the uplink communication in a multi-cell LoRa system is measured in terms of the success probability and the potential throughput.

The contributions of this paper are as follows: we present an analytical model of the intra- and inter-cell interference for the uplink communication in a multi-cell LoRa network employing quasi-orthogonal SFs in each cell; The inter-cell interference is derived first by finding the expression of distance distribution between a fixed point and random point inside an annulus. Subsequently, we use the intra- and inter-cell interference analysis to calculate and compare the success probability under two types of gateways distributions.

The rest of this paper is organized as follows: Section II introduces a stochastic geometry model for a multi-cell LoRa network. The expression for the success probability is derived in Section III. The results of the analytical model are presented in Section IV and conclusions are given in Section V.

II. Multi-Cell Uplink Model

In this section, we describe a model for uplink communication in a multi-cell LoRa system. We assume that a LoRa cell is a disk of radius R, in an Euclidean plane, with a gateway at its center. A gateway is the receiver of all the uplink traffic from the end devices (EDs) in a cell. For simplicity, we assume that all cells have the same radius and contain the same average number of EDs. Because of the ALOHA-based MAC, EDs randomly and independently access the channel. However, transmissions of each ED must satisfy the duty cycle constraint α imposed in the channel frequency band by regional regulations. Each ED is assigned a spreading factor (SF) which we assume depends only on the distance between an ED and its gateway.

The EDs are spatially distributed in an Euclidean plane according to two types of cluster processes: a Matèrn cluster process; and a Cox cluster process. In a Matèrn cluster process, the clusters are distributed according to a PPP and the devices inside each clusters are also distributed according to an independent PPP [10]. Matèrn cluster process can model the randomly and independently deployed LoRa gateways. Thanks to the properties of PPP, Matèrn cluster process lead to a simple mathematical formulation. Alternatively, if the cluster distribution is modelled using a MHC and the devices inside each cluster are distributed according to an independent PPP, the resulting point process is called a Cox cluster process [10]. MHC allows to model a minimum distance between clusters (i.e. hard-core distance). In our model, the hard-core distance is the minimum distance between each pair of LoRa gateways. This minimum distance can be due to physical constraints (i.e. availability of locations where to deploy the gateways) and/or due to specific network planning. This characteristic makes MHC more suited to model realistic cell planning than PPP. Unfortunately, MHC leads to a mathematical formulation lacking a closed form solution but it still allows to find a tight lower [11]. In the following sections we present the mathematical formulation for a model of a multi-cell LoRa system, for both MHC and PPP distributed gateways. We leave the choice on how to determine which of the two distributions best describes a specific LoRa multi-cell system to the readers.

A. Matèrn Cluster Point Process

It is assumed that the gateways are homogeneously distributed according to a Poisson point process (PPP) ϕ_G, of intensity $\lambda_G > 0$. In a generic cell i of radius R which we denote with $\mathcal{B}(i, R)$, the EDs are homogeneously distributed according to a PPP $\phi_{L,i}$ of intensity $\lambda_L > 0$. The union of all PPP $\phi_{L,i}$ form a Matèrn cluster process. The probability density function (PDF) of the distance of an offspring point (i.e. ED) from its parent point (i.e gateway) is given by

$$f_R(r) = \begin{cases} \frac{2r}{R^2} & \text{for } r \leq R; \\ 0 & \text{otherwise.} \end{cases} \tag{1}$$

The average number of EDs in a cell is given by $N = \lambda_L \pi R^2$. Assuming that all EDs transmit on the channel with the duty cycle α, the average number of EDs simultaneously active in a cell is αN. Let K be the cardinality of the set $\mathcal{K}$ of available SFs in LoRa. A cell $\mathcal{B}(i, R)$ can be divided into K annuli, each populated by EDs using the same SF, as showed in Fig. 2.

B. Matèrn Hard-core Point Process

In planned networks, the gateways are usually not placed independently from each other. The gateways are typically deployed such that the coverage area is maximized while the overlap between the cells is minimized. To model this scenario, we assume that the LoRa gateways are distributed according to a Matèrn hard-core process (MHC). A MHC is generated from a homogeneous PPP ϕ_P, of intensity $\lambda_P > 0$ to which a probabilistic thinning is applied that is dependent on the underlying process. In this paper, we use the Matèrn I hard-core process in which the thinning rule is to remove the points that are closer than a hard-core distance. Matèrn I processes are typically used in wireless systems to model CSMA/CA-based networks or the repulsions in the deployment of neighboring wireless nodes. Let d be the hard-core distance between two points of a Matèrn I process, then the probability of retaining an arbitrary point from the original PPP ϕ_P is given by [11]

$$p = \frac{1 - \exp\left(-\lambda_P \pi d^2\right)}{\lambda_P \pi d^2}. \tag{2}$$

The resulting density of the Matèrn I process, λ_G, is $\lambda_G = \lambda_P \cdot p$. In our scenario, we assume that the hard-core distance is equal to the cell radius (i.e. $d = R$).

C. Channel Model

We assume that all EDs transmit on the same channel with bandwidth BW and carrier frequency f_c. We model the channel as a Rayleigh block-fading with additive white Gaussian noise (AWGN) and free space path loss (FSPL). The variance of the AWGN is $\sigma^2 = -174 + \text{NF} + 10\log\text{BW}$ [dBm], where NF is the noise figure of the receiver. Let $s_1(t, \text{SF}_p)$ be the desired signal transmitted to a gateway y_0 by ED $x_{0,1}$ using SF p. The signal is affected by the block fading with coefficient $h(t)$. The received signal $r(t)$ at the gateway y_0, is given by

$$\begin{aligned} r(t) &= \gamma \|x_{0,1}\|^{-\eta} h(t) * s_{0,1}(t, SF_p) + n(t) \\ &+ \sum_{j=2}^{N_{SF_p}} \mathbb{1}_j^{SF_p} \gamma \|x_{0,j}\|^{-\eta} g_{0,j}(t) * s_{0,j}(t, SF_p) \\ &+ \sum_{q \in \mathcal{K} \setminus p} \sum_{k=1}^{N_{SF_q}} \mathbb{1}_k^{SF_q} \gamma \|x_{0,k}\|^{-\eta} g_{0,k}(t) * s_{0,k}(t, SF_q) \\ &+ \sum_{y \in \phi_G \setminus y_0} \sum_{q \in M} \sum_{k=1}^{N_{SF_q}} \mathbb{1}_k^{SF_q} \gamma \|x_{i,k} + y_i\|^{-\eta} g_{i,k}(t) * s_{i,k}(t, SF_q), \end{aligned} \tag{3}$$

where $n(t)$ is the AWGN with zero mean and variance σ^2; $\|x_{i,k}\|$ is the distance between ED k in cell i and its gateway y_i; $\|y_i\|$ is the distance between gateway y_i and gateway y_0; $g_{i,k}(t)$ is the fading coefficient for the interfering EDs in cell i; γ and η are, respectively, the frequency dependent factor and

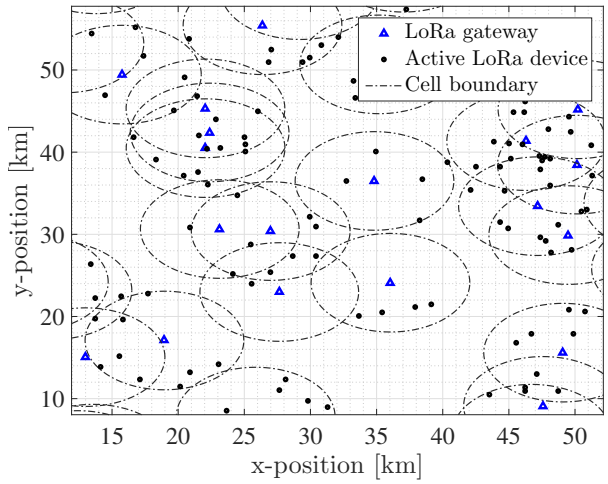

(a) An example deployment of LoRa networks according to Matèrn cluster process with parameters: $\lambda_G = 8.8{\cdot}10^{-3}$ points/km^2, $\lambda_L \simeq 4.4 \cdot 10^{-2}$ points/km^2 and $R = 6$ km.

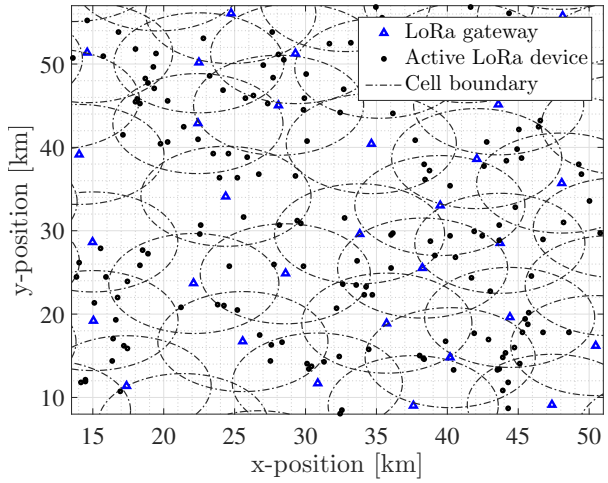

(b) An example deployment of LoRa cells according to a Matèrn hard-core point process of type I for the gateways and a PPP for the LoRa devices, with $\lambda_G = 8.8 \cdot 10^{-3}$ points/km^2, $\lambda_L \simeq 4.4 \cdot 10^{-2}$ points/km^2 and $R = 6$ km.

Fig. 1. Realization of the stochastic geometry models for a multi-cell LoRa system: (a) Poisson cluster process; (b) Cox cluster process with MHC for the cells.

the path loss exponent; N_{SF_p} is the number of EDs with SF p in a cell; $\mathbb{1}_k^{SF_p}$ is an indicator function for ED $x_{i,k}$ transmitting with SF p. A visual representation of the distances $\|x_{0,j}\|$ and $\|x_{i,k} + y_i\|$ can be found in Fig. 2.

In (3), the received signal at the gateway is the sum of multiple terms: the first, is the desired signal; the second is the noise; the third is the interference generated by EDs in the same cell and using the same SF; the fourth is the interference caused by EDs in the same cell and of different SF and the last term is the interference caused by EDs in different cells.

D. SNR and SIR Calculation

For the channel and signal models presented in Section II-C, the signal-to-noise ratio (SNR) for a signal transmitted by

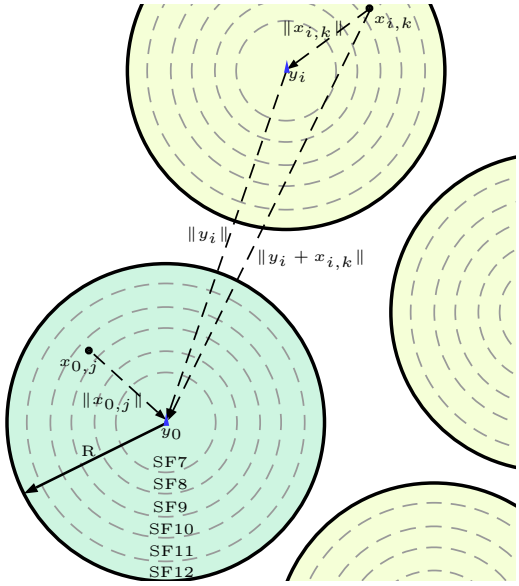

Fig. 2. A representation of the LoRa multi-cell scenario.

ED $x_{0,k}$ to the reference gateway y_0 is given by

$$\text{SNR}(x_{0,k}) = \frac{p_t H \gamma \|x_{0,k}\|^{-\eta}}{\sigma^2}, \tag{4}$$

where: p_t is the transmitting power, and $H := |h|^2$ is the channel gain between ED $x_{0,k}$ and its gateway.

From (3), we can write the signal-to-interference ratio (SIR) for a signal transmitted by ED $x_{0,k}$ to the reference gateway y_0 under interference from SF q as

$$\text{SIR}(x_{0,k}, q) = \frac{p_t H \gamma \|x_{0,k}\|^{-\eta}}{\sum\limits_{y_i \in \phi_G} \sum\limits_{x_j \in \phi_{L,i,q}} p_t G_{i,j} \gamma \|x_{i,j} + y_i\|^{-\eta}}, \tag{5}$$

where $\phi_{L,i,q}$ is the PPP of the ED with SF q in cell i; $G_{i,j} = |g_{i,j}|^2$ the channel gain between ED $x_{i,j}$ of cell i and the reference gateway y_0.

In (5), the interference term at the denominator can be written as the sum of two contributions: the intra-cell interference $\mathcal{I}^q_{\text{intra}}$ from SF q, generated by EDs in annulus q of the cell $\mathcal{B}(0, R)$ and the inter-cell interference $\mathcal{I}^q_{\text{inter}}$ from SF q, generated by EDs in annulus q of the remaining cells $\mathcal{B}(i, R)$ with $i \neq 0$. The expressions for intra- and inter-cell interference are respectively

$$\mathcal{I}^q_{\text{intra}} = \sum_{x_{0,j} \in \phi_{L,0,q}} p_t G_{0,j} \gamma \|x_{0,j}\|^{-\eta}, \tag{6}$$

$$\mathcal{I}^q_{\text{inter}} = \sum_{y_i \in \phi_G \setminus y_0} \sum_{x_{i,j} \in \phi_{L,i,q}} p_t G_{i,j} \gamma \|x_{i,j} + y_i\|^{-\eta}. \tag{7}$$

The overall interference is the sum of the intra- and inter-cell interference from each SF, given by

$$\mathcal{I} = \sum_{q \in \mathcal{K}} \left(\mathcal{I}^q_{\text{intra}} + \mathcal{I}^q_{\text{inter}}\right). \tag{8}$$

E. Distance Distribution

In order to determine the system performance, we need an expression of the distance distribution of the EDs from the gateways. The usefulness of the distance distribution to simplify the interference calculation in a multi-cell network was highlighted in [12]. In LoRa, the SF plays a significant role in the interference calculation, the PDF of the distance between EDs and gateway must be found for each of the SFs. The PDF of the distance between an ED and the gateway of its cell is given by (1). The PDF of the distance between the EDs in a cell and a gateway of a different cell can be derived using geometric probability. In geometric terms, we want to find the PDF of the distance between a fixed point outside an annulus (i.e. gateway) and a random point inside the annulus (i.e. ED). Given two gateways separated by distance y, the pdf of the distance of an ED with SF q in the first cell from the gateway of the second cell, is given by

$$f_d(x,y,q) = \frac{2x\left(\beta_2 - \beta_1\right)}{\pi\left(l_q^2 - l_{q-1}^2\right)} \text{ for } y + l_q \leq x \leq y + l_q, \quad (9)$$

where: l_q and l_{q-1} are, respectively, the radii of the outer and inner rings of the annulus formed by the EDs with SF q; β_2 and β_1 are trigonometric functions of the parameters y, l_q and l_{q-1} given by

$$\beta_2 = \cos^{-1}\left(\frac{x^2 + y^2 - l_q^2}{2yx}\right);\ \beta_1 = \cos^{-1}\left(\frac{x^2 + y^2 - l_{q-1}^2}{2yx}\right) \quad (10)$$

The derivation of (9) and (10) can be found in Appendix A.

A limitation to the analytical model presented in this work is that the cell coverage area is assumed to be a disk. Considering coverage areas other than a disk would increase the geometric complexity of the region of space where LoRa EDs using the same SF are located. This, in turn, would increase the complexity of the probability density function of the distance between gateway and EDs. For this reason, the commonly used assumption that devices are connected to the nearest gateway cannot be applied here, as this would result in Voronoi cells.

III. Success Probability

Let $\|x_1\|$ be the distance between ED x_1 with SF p and its gateway. Let $\delta_{q,p}$ [dB] be the SIR threshold needed for successfully decoding the message transmitted by an ED using SF p under interference from the EDs transmitting using SF q. Also, let θ_p [dB] be the SNR threshold needed for successfully decode the message transmitted by an ED using SF p in the presence of AWGN. Then, the success probability for ED x_1 using SF p is given by

$$\begin{aligned} &P_{\text{suc}}(x_1,p) = \\ &\mathbb{P}\left[\left\{\bigcap_{q\in\mathcal{K}}\{\text{SIR}(x,q) \geq \delta_{p,q}\}\right\}\bigcap\{\text{SNR}(x) \geq \theta_p\}\middle| x = x_1\right] \\ &\geq \mathbb{P}\left[\text{SNR}(x_1) \geq \theta_p\right]\prod_{q\in\mathcal{K}}\mathbb{P}\left[\text{SIR}(x_1,q) \geq \delta_{p,q}\right], \end{aligned} \quad (11)$$

where the inequality comes from [6, eq. (5)]. Thanks to (11), we can calculate the lower bound on the success probability by calculating the probability that the conditions on the SNR and SIR are independently satisfied.

The probability that the SNR of a message transmitted to the gateway by ED x_1 using SF p is above the threshold θ_p, is given by

$$\begin{aligned} \mathbb{P}\left[\text{SNR}(x_1) \geq \theta_p\right] &= \mathbb{P}\left[H \geq \frac{\sigma^2\theta_p}{p_t\gamma\|x_1\|^{-\eta}}\right] \\ &\overset{(a)}{=} \exp\left(-\frac{\sigma^2\theta_p}{p_t\gamma\|x_1\|^{-\eta}}\right), \end{aligned} \quad (12)$$

where (12.a) is obtained by using the generating function of exponential random variable $H \sim \exp(1)$.

The probability that the SIR of a message transmitted to the gateway by ED x_1 using SF p and affected by interference from EDs using SF q is above the threshold $\delta_{q,p}$, is given by

$$\begin{aligned} &\mathbb{P}\left[\text{SIR}(x_1,q) \geq \delta_{p,q}\right] = \mathbb{P}\left[H \geq \frac{\delta_{p,q}\left(\mathcal{I}^q_{\text{intra}} + \mathcal{I}^q_{\text{inter}}\right)}{p_t\gamma\|x_1\|^{-\eta}}\right] \\ &= \mathbb{E}_{\mathcal{I}^q_{\text{inter}}}\left[\exp\left(-\frac{\delta_{p,q}\mathcal{I}^q_{\text{inter}}}{p_t\gamma\|x_1\|^{-\eta}}\right)\right]\mathbb{E}_{\mathcal{I}^q_{\text{intra}}}\left[\exp\left(-\frac{\delta_{p,q}\mathcal{I}^q_{\text{intra}}}{p_t\gamma\|x_1\|^{-\eta}}\right)\right] \\ &= \mathcal{L}_{\mathcal{I}^q_{\text{inter}}}(s)\cdot\mathcal{L}_{\mathcal{I}^q_{\text{intra}}}(s), \end{aligned} \quad (13)$$

where $s = \frac{\delta_{p,q}}{\gamma p_t\|x_1\|^{-\eta}}$.

By substituting (12) and (13) in (11), we obtain the lower bound to the success probability

$$\begin{aligned} P_{\text{suc}}(x_1,p) \geq &\exp\left(-\frac{\sigma^2\theta_p}{p_t\gamma x_1^{-\eta}}\right) \\ &\times\prod_{q\in\mathcal{K}}\mathcal{L}_{\mathcal{I}^q_{\text{intra}}}\left(\frac{\delta_{p,q}}{\gamma p_t\|x_1\|^{-\eta}}\right)\mathcal{L}_{\mathcal{I}^q_{\text{inter}}}\left(\frac{\delta_{p,q}}{\gamma p_t\|x_1\|^{-\eta}}\right). \end{aligned} \quad (14)$$

From the success probability P_{suc}, we are able to calculate the connection probability, that is the probability that a generic ED in an annulus can successfully transmit its packet to the gateway. We express the average connection probability of a LoRa ED with SF p as

$$P_{\text{conn}}(p) = \int_{l_{p-1}}^{l_p} P_{\text{suc}}(r,p)\cdot\frac{2r}{l_p^2 - l_{p-1}^2}dr. \quad (15)$$

To find P_{suc} and P_{conn}, the Laplace transform (LT) for both intra- and inter-cell interference needs to be found.

A. Intra-cell Interference

In case of intra-cell interference from SF q, the LT $\mathcal{L}_{\mathcal{I}^q_{\text{intra}}}(s)$ can be obtained as in [6] and [8]. The LT of $\mathcal{I}_{\text{intra}}$ is given by

$$\begin{aligned} \mathcal{L}_{\mathcal{I}^q_{\text{intra}}}(s) &= \mathbb{E}_{\phi_{L,0},G}\left[exp\left(-s\mathcal{I}_{\text{intra}}\right)\right] \\ &= \exp\left(-2\pi\lambda_L\alpha\int_{l_{q-1}}^{l_q}\frac{sp_t\gamma x^{-\eta}}{1 + sp_t\gamma x^{-\eta}}xdx\right). \end{aligned} \quad (16)$$

where α is the activity factor, that is the percentage of time that an ED can transmit on the channel.

B. Inter-cell Interference

In case of inter-cell interference, the procedure to find the LT changes depending on the distribution of the gateways.

$$
\begin{aligned}
\mathcal{L}^{I}_{\mathcal{I}^q_{\text{inter}}}(s) &= \mathbb{E}_{\phi_G,\phi_{L,i},G}\left[exp\left(-s\mathcal{I}^q_{\text{inter}}\right)\right] \\
&= \mathbb{E}_{\phi_G,\phi_{L,i},G_{i,j}}\left[\exp\left(-s\sum_{y_i\in\phi_G\setminus y_0}\sum_{x_j\in\phi_{L,i}} p_t G_{i,j}\gamma\|x_{i,j}+y_i\|^{-\eta}\right)\right] \\
&= \mathbb{E}_{\phi_G,\phi_{L,i},G_{i,j}}\left[\prod_{y_i\in\phi_G\setminus y_0}\prod_{x_j\in\phi_{L,i}} \exp\left(-sp_t G_{i,j}\gamma\|x_{i,j}+y_i\|^{-\eta}\right)\right] \\
&\overset{(a)}{=} \mathbb{E}_{\phi_G,\phi_{L,i}}\left[\prod_{y_i\in\phi_G\setminus y_0}\prod_{x_j\in\phi_{L,i}} \frac{1}{1+sp_t\gamma\|x_{i,j}+y_i\|^{-\eta}}\right] \\
&\overset{(b)}{=} \mathbb{E}_{\phi_G}\left[\prod_{y_i\in\phi_G\setminus y_0} \exp\left(-\alpha\lambda_L\pi(l_q^2-l_{q-1}^2)\int_{\mathbb{R}^2}\frac{sp_t\gamma x^{-\eta}}{1+sp_t\gamma x^{-\eta}} f_d(x,y_i,q)dx\right)\right] \\
&\overset{(c)}{=} \mathbb{E}_{\phi_G}\left[\prod_{y_i\in\phi_G\setminus y_0} \exp\left(-\alpha\lambda_L\pi(l_q^2-l_{q-1}^2)\int_{y_i-l_q}^{y_i+l_q}\left(\frac{\delta_{p,q}x^{-\eta}}{\delta_{p,q}x_1^{-\eta}+x^{-\eta}}\right) f_d(x,y_i,q)dx\right)\right] \\
&\overset{(d)}{=} \exp\left[-2\pi\lambda_G\int_0^{\infty}\left[1-\exp\left(-\alpha\lambda_L\pi(l_q^2-l_{q-1}^2)\int_{y-l_q}^{y+l_q}\left(\frac{\delta_{p,q}x^{-\eta}}{\delta_{p,q}x_1^{-\eta}+x^{-\eta}}\right) f_d(x,y,q)dx\right)\right] ydy\right].
\end{aligned}
\tag{17}
$$

1) Matern cluster point process: In case of Matern cluster point process, as stated in Section II, the gateways are distributed according to a PPP ϕ_G and the LT of the inter-cell interference, $\mathcal{L}^{I}_{\mathcal{I}_{\text{inter}}}(s)$, is given by (17). Eq. (17.a) is obtained by using the generating function of exponential random variable $G \sim \exp(1)$. Using the probability generating functional (PGFL) of the homogeneous PPP, $\phi_{L,1}$, (17.b) is obtained. Transforming the integral from Cartesian to polar coordinates and integrating over the support of $f_d(x, y_i, q)$ gives (17.c). Finally, (17.d) is obtained by using the PGFL of the homogeneous PPP ϕ_G.

2) Matèrn Hard-core Point Process: When the gateways are distributed according to a MHC, the expression of the LT for the inter-cell interference is no longer valid, since (17.d) is obtained by using the PGFL of an homogeneous PPP. Let $\Gamma(y_i)$ be the inner function in the integral in (17.c), given by

$$
\begin{aligned}
\Gamma(y_i,q) = &-\alpha\lambda_L\pi(l_q^2-l_{q-1}^2) \\
&\times\int_{y_i-l_q}^{y_i+l_q}\left(\frac{\delta_{p,q}x^{-\eta}}{\delta_{p,q}x_1^{-\eta}+x^{-\eta}}\right) f_d(x,y_i,q)dx.
\end{aligned}
\tag{18}
$$

Jensen's inequality can be applied to the expectation of the MHC ϕ_G in (17.c), to obtain a lower bound of the LT of the inter-cell interference

$$
\begin{aligned}
\mathcal{L}^{II}_{\mathcal{I}^q_{\text{inter}}}(s) &= \mathbb{E}_{\phi_G}\left[\prod_{y_i\in\phi_G\setminus y_0}\exp\left(\Gamma(y_i,q)\right)\right] \\
&= \mathbb{E}_{\phi_G}\left[\exp\left(\sum_{y_i\in\phi_G\setminus y_0}\Gamma(y_i,q)\right)\right] \\
&\geq \exp\left(\mathbb{E}_{\phi_G}\left[\sum_{y_i\in\phi_G\setminus y_0}\Gamma(y_i,q)\right]\right).
\end{aligned}
\tag{19}
$$

To solve the expectation over the MHC ϕ_G in (19), we use the approach presented in [11], based on the following property. Let $f(x) : \mathbb{R}^2 \to [0,\infty]$ be an integrable function and ϕ_G a point process, then

$$
\begin{aligned}
\mathbb{E}_{\phi_G}\left[\sum_{y_i\in\phi_G} f(y_i)\right] &= \frac{1}{\lambda}\int_{\mathbb{R}^2}\rho^{(2)}(y)f(y)dy \\
&= \frac{2\pi}{\lambda}\int_0^{\infty}\rho^{(2)}(y)f(y)ydy,
\end{aligned}
\tag{20}
$$

where $\rho^{(2)}$ is the second order product density of a MHC of intensity λ_G and hard-core distance R, given by

$$
\rho^{(2)}(u) = \begin{cases}
\lambda_G^2 & \text{if } u \geq 2R \\
\frac{2\left[1-\exp\left(-\lambda_p\pi R^2\right)\right]}{\pi R^2[V(u)-\pi R^2]} - \frac{2[1-\exp(-\lambda_p V(u))]}{V(u)[V(u)-\pi R^2]} & \text{if } R \leq u \leq 2R \\
0 & \text{otherwise}
\end{cases}
\tag{21}
$$

where $V(u)$ is the area of the union of two disks of radius R with centres separated by u, and given by

$$
V(u) = 2\pi R^2 - 2R^2\text{arcos}\left(\frac{u}{2R}\right) + u\sqrt{R^2-\frac{u^2}{4}}.
$$

Combining (19) and (20) we obtain a lower bound on the LT of the inter-cell interference:

$$
\mathcal{L}_{\mathcal{I}^q_{\text{inter}}}(s) \geq \exp\left(\frac{2\pi}{\lambda_G}\int_0^{\infty}\rho^{(2)}(y)\Gamma(y,q)ydy\right). \tag{22}
$$

IV. Results Analysis

We evaluate the uplink success and connection probability of a LoRa link for different intensities of the cluster point process. We compare the results obtained when the gateways are distributed according to a PPP and a MHC. For

having a fair comparison the results obtained from using the PPP and the MHC must be compared for the same intensity λ_G. From the constraint on the minimum distance between points in a MHC, we derive a constraint on the maximum intensity of the point process. For a MHC with hard-core distance $d = 6$ km, the maximum intensity is $\lambda_G^{\text{MAX}} = \left(\pi d^2\right)^{-1} \cong 8.84 \cdot 10^{-3}$points/km^2. We assume that the average number of EDs in each cell is $N = 1500$. The cell radius is $R = 6$ km, in accordance with dense urban deployment [1]. The parameters for the analytical model are given in Table I, whereas the SF specific parameters are given in Table II. We select carrier frequency, bandwidth and activity factor for a LoRaWAN network operating under Europe's *ETSI EN 300 220* regulations. The SF intervals $[l_{p-1}, l_p]$ are assigned using an equal-interval-based (EIB) scheme [6].

TABLE I
LORA PARAMETERS USED FOR THE PERFORMANCE EVALUATION

Parameter	Symbol	Value
Bandwidth	BW	125 kHz
Carrier Frequency	f_c	868 MHz
Noise Power Density	N_0	-174 dBm/Hz
Noise Figure	NF	6 dBm
Transmit power	p_t	19 dBm
Activity Factor	α	0.33 %
Pathloss exponent	η	$\in [2.1, 2.9]$
Cell Radius	R	6 km
MHC Hard-core distance	d	6 km

TABLE II
SPREADING FACTORS PARAMETERS

SF	Radii $l_{p-1} - l_p$	SNR Th. θ_p	Data rate $DR(p)$
SF_7	$0 - 1$ km	-6 dB	5468 bps
SF_8	$1 - 2$ km	-9 dB	3125 bps
SF_9	$2 - 3$ km	-12 dB	1757 bps
SF_{10}	$3 - 4$ km	-15 dB	977 bps
SF_{11}	$4 - 5$ km	-17.5 dB	537 bps
SF_{12}	$5 - 6$ km	-20 dB	293 bps

The values of the SIR threshold $\delta_{p,q}$ for the six SFs of LoRa are derived from [13] which are

$$\Delta_{[dB]} = \begin{array}{c} \begin{matrix} \text{SF}_7 & \text{SF}_8 & \text{SF}_9 & \text{SF}_{10} & \text{SF}_{11} & \text{SF}_{12} \end{matrix} \\ \begin{pmatrix} 1 & -8 & -9 & -9 & -9 & -9 \\ -11 & 1 & -11 & -12 & -13 & -13 \\ -15 & -13 & 1 & -13 & -14 & -15 \\ -19 & -18 & -17 & 1 & -17 & -18 \\ -22 & -22 & -21 & -20 & 1 & -20 \\ -25 & -25 & -25 & -24 & -23 & 1 \end{pmatrix} \end{array} \begin{matrix} \text{SF}_7 \\ \text{SF}_8 \\ \text{SF}_9 \\ \text{SF}_{10} \\ \text{SF}_{11} \\ \text{SF}_{12} \end{matrix} \tag{23}$$

Fig. 3 shows the success probability of a LoRa ED for different cell densities, which is calculated using (18). In Fig. 3a the cells are distributed according to a PPP whereas in Fig. 3b the cells are distributed accordingly to a MHC. For comparison, the success probability in a single LoRa cell is also shown, which is obtained by removing the inter-cell interference $\mathcal{I}^q_{\text{inter}}$ from the model. The typical reverse sawtooth shape of the success probability previously highlighted in [4] can still be observed under a multi-cell LoRa network architecture. This shape is the consequence of the different SNR and SIR thresholds of LoRa SFs. The sharp increase in success probability correspond to a next annulus of the cell where a higher SF is used. At low value of λ_G the success probability for the PPP and the MHC are very similar. As the cell density increases, the success probability decreases more prominently for ED located farther away from the gateway. The success probability in cells distributed according to a PPP offers a lower bound to the success probability in cell distributed accordingly to a MHC. The bound is tight for low cell density, before gradually becoming looser at increasing cell density. Another effect of increasing the cell density on the success probability is the gradual disappearance of the sawtooth shape. The factor that contributes the most to this is the choice of the SF intervals in the cell. For obtaining these results, the SF intervals are assigned using an equal-interval-based (EIB) scheme [5]. In EIB, the cell radius is divided in equal sized intervals as shown in Table II. This scheme causes the annulus of higher SFs to occupy a larger share of the cell area, which leads to a larger share of EDs using higher SFs.

At low cell-density, the increase in co-SF interference affecting the ED using higher SF is more than being compensated by a decrease in SIR threshold for the inter-SF interference. At high cell-density, the increase in co-SF interference causes a sharp decline in the success probability in particular for low SF. This is because the difference in the size of the ED population of smaller SF is much significant; for example in a cell using EIB scheme the number of ED using SF7 is three times the number of ED using SF1, whereas the number of EDs using SF12 is only $11/9$ the number of ED using SF11. The success probability of cells distributed accordingly to a PPP is most affected by this behavior. Fig. 3a at the distance of 1 km (i.e. boundary between SF7 and SF8 annulus) offers a clear example. To confirm this observation, we calculated the success probability with an equal-area-based (EAB) scheme which assures that each SFs is allocated to an equal number of EDs. In this case we noticed that as expected the characteristic sawtooth shape is present for any cluster intensity.

Fig. 4 shows the average connection probability of each SF for different cell densities, calculated using (15). Fig. 4a is for the case of cells distributed according to PPP, while Fig. 4b is for cells distributed according to MHC. We can observe that when the cells are distributed as a MHC, the connection probability of the EDs closer to the gateway and using smaller SFs are not particularly affected by the cell density. Using a MHC distribution results in a significant improvement of the connection probability for EDs that are located farther away from the gateway compared to a PPP distribution.

A possible solution to this problem is to change the way SF are allocated. Instead of an EIB scheme, other schemes like [5] could be used to maximize the average success probability. A comparison between the results obtained using the PPP and using the MHC shows significant difference for high cluster intensity. Particularly the performance of the ED when cluster are distributed according to a PPP are worse for all the SF.

The area spectral efficiency (ASE) is often used in stochastic geometry as a measure of the total network throughput.

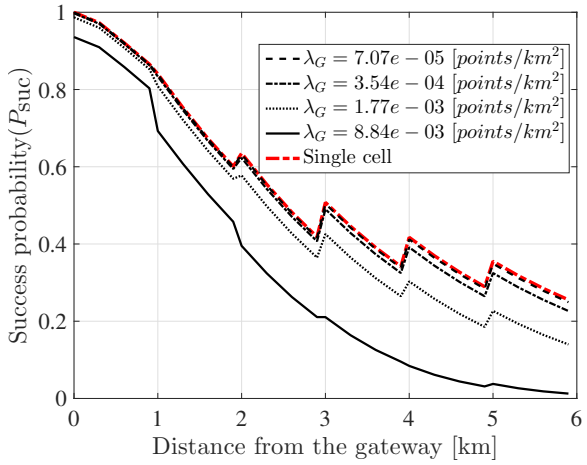

(a) Poisson point process, with intensity λ_G.

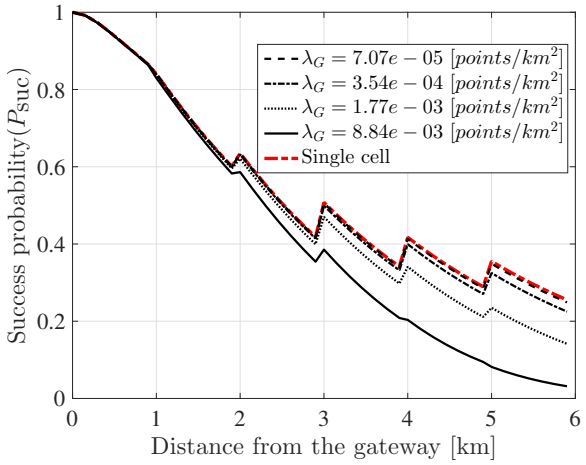

(b) Matèrn hard-core point process of type I, with intensity λ_G and hard-core distance $d \equiv R = 6$km.

Fig. 3. Success probability in a LoRa cell with $R = 6$ km, $\alpha = 0.33\%$ and $N = 1500$. The cell are distributed accordingly to: (a) Poisson point process; (b) Matèrn hard-core point process of type I

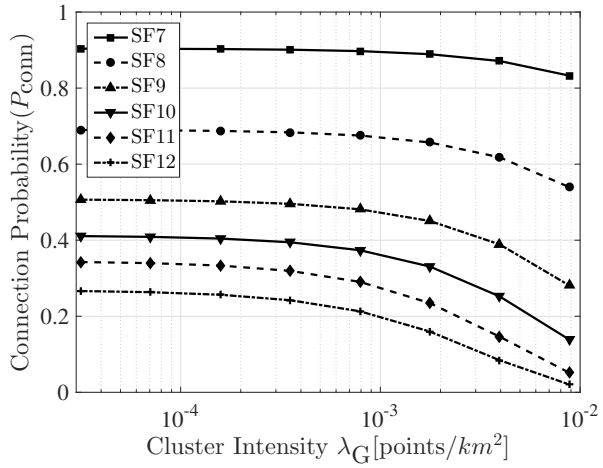

(a) Poisson point process, with intensity λ_G.

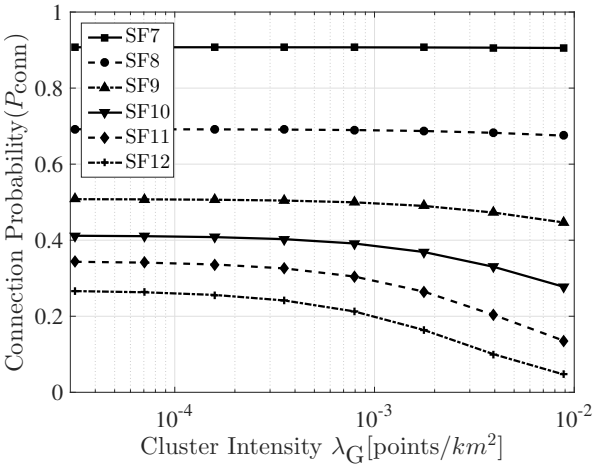

(b) Matèrn hard-core point process of type I, with intensity λ_G and hard-core distance $d \equiv R = 6$km.

Fig. 4. Connection probability in a LoRa cell with $R = 6$ km, $\alpha = 0.33\%$ and $N = 1500$. The cell are distributed accordingly to: (a) Poisson point process; (b) Matèrn hard-core point process of type I.

LoRaWAN describes the adaptive data rate (ADR) mechanism for optimizing the allocation of SF and transmission power with respect to the channel conditions. An ED can optionally decide to use the ADR mechanism to adapt its SF and transmit power according to the measured SNR. In this work, the SFs are assumed to be fixed and are allocated accordingly to the distance between the EDs and the gateway. Because the transmission rate is fixed and does not depend on the channel state, a better throughput performance metric is the average potential throughput. We define the average potential throughput of SF p as the average number of bits transmitted per unit time per unit bandwidth per unit area. The average potential throughput can be directly obtained from the connection probability

$$\mathbb{E}\left[S\left(p\right)\right] = \pi\alpha\lambda_L\left(l_p^2 - l_{p-1}^2\right)\lambda_G P_{\text{conn}}(p)\tau(p), \qquad (24)$$

where $\pi\alpha\lambda_L\left(l_p^2 - l_{p-1}^2\right)\lambda_G$ is the average density of the active EDs with SF p, $P_{\text{conn}}(p)$ is given by (11) and $\tau(p)$ is the spectral efficiency calculated as the ratio between data rate DR and channel bandwidth BW. The average potential throughput assumes that the transmission occurs with a constant rate $DR(p)$ which does not depend on the channel state. Then the messages are successfully decoded at the receiver if both the conditions on the SIR and SNR are met. Fig. 5 shows the potential throughput when the gateways are distributed according to a PPP and a MHC for different clusters intensity. At low cluster intensity both PPP and MHC show a linear increase in the potential throughput. The relation became sub-linear for higher cluster intensities.

V. Conclusions

In this work, an analytical model based on stochastic geometry is proposed to study the performance of a multi-cell LoRa system. We model the interference from the same and different spreading factors, as well as the inter- and intra-cell

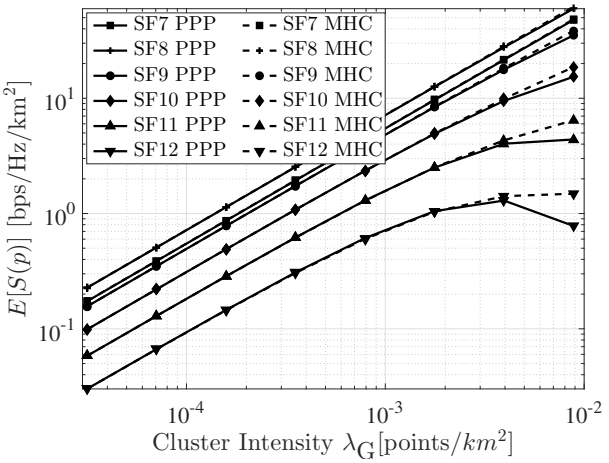

Fig. 5. Potential throughput for different cluster intensity λ_G.

interference, in order to calculate the aggregated interference at a gateway. In order to describe the inter-cell interference easily, we derived the distance distribution between the gateway in a cell and an annulus of a different cell. To allow the study of both unplanned and planned cell deployment, the distribution of the cluster was modelled using a PPP and a MHC. The model presented in this paper could provide some help in the designs and planning of LoRa cells in dense deployment scenarios. The results show how the impact of inter-cell cause a non-negligible performance degradation, particularly for high SFs. In the case of single cell LoRa, the average success probability of the EDs using SF_{12} is 29.5% of the success probability of EDs using SF_7, whereas the same ratio decreases to 22% in a multi-cell scenario with $\lambda_G = 10^{-3}$. We argue that the negative effect on performance can be reduced with a proper SF allocation scheme which would take into account not only the interference from devices within a cell but also the interference from neighboring cells.

REFERENCES

[1] M. Centenaro, L. Vangelista, A. Zanella, and M. Zorzi, "Long-range communications in unlicensed bands: the rising stars in the IoT and smart city scenarios," *IEEE W. Commun.*, vol. 23, no. 5, pp. 60–67, October 2016.

[2] Semtech Corporation, "AN1200.22 LoRa™ Modulation Basics," https://www.semtech.com/uploads/documents/an1200.22.pdf, 2015, [Online; accessed 7-June-2018].

[3] LoRa Alliance Technical Committee, "LoRaWAN 1.1 Specification," https://lora-alliance.org/sites/default/files/2018-04/lorawantm_specification_-v1.1.pdf, 2017, [Online; accessed 13-June-2018].

[4] O. Georgiou and U. Raza, "Low power wide area network analysis: Can LoRa scale?" *IEEE W. Commun. Lett.*, vol. 6, no. 2, pp. 162–165, 2017.

[5] Z. Qin, Y. Liu, G. Y. Li, and J. A. McCann, "Modelling and analysis of low-power wide-area networks," in *IEEE ICC, 2017*, 2017, pp. 1–7.

[6] J.-T. Lim and Y. Han, "Spreading Factor Allocation for Massive Connectivity in LoRa Systems," *IEEE Commun. Lett.*, vol. 22, no. 4, pp. 800–803, 2018.

[7] D. Croce, M. Gucciardo, I. Tinnirello, D. Garlisi, and S. Mangione, "Impact of spreading factor imperfect orthogonality in LoRa communications," in *International Tyrrhenian Workshop on Digital Communication*. Springer, 2017, pp. 165–179.

[8] A. Mahmood, E. Sisinni, L. Guntupalli, R. Rondon, S. A. Hassan, and M. Gidlund, "Scalability Analysis of a LoRa Network under Imperfect Orthogonality," *IEEE Trans. Ind. Informat.*, 2018, doi: 10.1109/TII.2018.2864681.

[9] H. ElSawy, E. Hossain, and M. Haenggi, "Stochastic geometry for modeling, analysis, and design of multi-tier and cognitive cellular wireless networks: A survey," *IEEE Commun. Surv. Tutor.*, vol. 15, no. 3, pp. 996–1019, 2013.

[10] M. Haenggi, *Stochastic geometry for wireless networks*. Cambridge University Press, 2012.

[11] A. M. Ibrahim, T. ElBatt, and A. El-Keyi, "Coverage probability analysis for wireless networks using repulsive point processes," in *IEEE PIMRC, 2013*, 2013, pp. 1002–1007.

[12] J. Tang, G. Chen, J. P. Coon, and D. E. Simmons, "Distance distributions for Matèrn cluster processes with application to network performance analysis," in *IEEE ICC, 2017*, 2017, pp. 1–6.

[13] D. Croce, M. Gucciardo, S. Mangione, G. Santaromita, and I. Tinnirello, "Impact of LoRa Imperfect Orthogonality: Analysis of Link-Level Performance," *IEEE Commun. Lett.*, vol. 22, no. 4, pp. 796–799, 2018.

[14] A. M. Mathai, *An introduction to geometrical probability: distributional aspects with applications*. CRC Press, 1999, vol. 1.

APPENDIX A
DISTANCE BETWEEN A FIXED POINT AND RANDOM POINTS INSIDE AN ANNULUS

The distribution of the distance between a fixed point and the random point inside an annulus can be found using the notions from geometrical probability. In particular, the following procedure can be derived as a special case of the distance between a fixed point outside and a random point inside a circle described in [14].

We consider the distribution of the distance between a random point B, independently and uniformly distributed inside the annulus of radii R_2 and R_1 and centred in O, and a fixed point A located outside the annulus. Let R be the length of the line $\overline{AO}$ and ρ the length of the line $\overline{AB}$. The distribution of ρ can be found from the area $S(\rho)$ in Fig. 6.

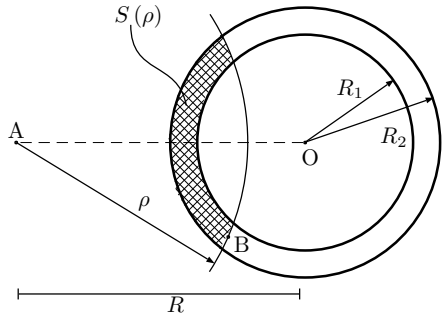

Fig. 6. Area $S(\rho)$ given by the intersection of the disk with center A and radius ρ and the annulus centred in O and with radii R_2, R_1.

The three disks in Fig. 6 have the following expressions

$$D_1 : x^2 + y^2 \leq R_1^2; \qquad D_2 : x^2 + y^2 \leq R_2^2;$$
$$D_3 : (x+R)^2 + y^2 \leq d^2.$$

The area $S(\rho)$ can be found as

$$S(\rho) = (D_3 \cap D_2) \setminus (D_3 \cap D_1). \tag{25}$$

The density function of the distance ρ is given by

$$f(\rho) = \frac{d}{d\rho}\frac{S(\rho)}{\pi(R_2^2 - R_1^2)} = \frac{2\rho(\beta_2 - \beta_1)}{\pi(R_2^2 - R_1^2)}, \tag{26}$$

where

$$\beta_2 = \cos^{-1}\left(\frac{\rho^2 + R^2 - R_2^2}{2R\rho}\right);\ \beta_1 = \cos^{-1}\left(\frac{\rho^2 + R^2 - R_1^2}{2R\rho}\right) \tag{27}$$